ACS OMEGA

Open Access

http://pubs.acs.org/journal/acsodf

Article

Neuronal Electrical Activity in Neuronal Networks Induced by a Focused Femtosecond Laser

Yumi Segawa, Wataru Minoshima, Kyoko Masui, and Chie Hosokawa*

Cite This: *ACS Omega* 2025, 10, 1354−1363

Read Online

ACCESS | Metrics & More | Article Recommendations | Supporting Information

ABSTRACT: The spatial propagation of neuronal activity within neuronal circuits, which is associated with brain functions, such as memory and learning, is regulated by external stimuli. Conventional external stimuli, such as electrical inputs, pharmacological treatments, and optogenetic modifications, have been used to modify neuronal activity. However, these methods are tissue invasive, have insufficient spatial resolution, and cause irreversible gene modifications. To establish neuronal stimulation with less invasiveness and higher spatial resolution, we propose and demonstrate single-neuron stimulation using a focused femtosecond laser. Fluorescence Ca^{2+} imaging and microelectrode array recordings of extracellular potentials revealed Ca^{2+} influx into the target neuron and high-frequency electrical responses after laser irradiation. These results indicate that femtosecond laser-induced neuronal electrical activity has a greater number of electrical spikes, lasts longer after stimulation, and propagates to a region more distant from the target neuron compared with the properties evoked by electrical stimulation. Focused femtosecond laser-induced stimulation can be a promising tool for stimulating single neurons in neuronal networks.

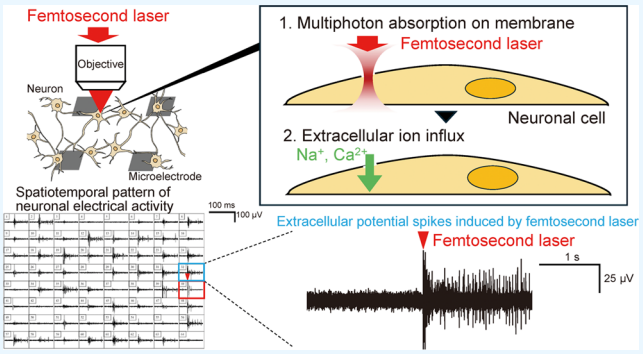

1. INTRODUCTION

In the human brain, 86 billion neurons form complex neuronal networks through synaptic connections and exhibit spontaneous electrical activity.[1] Action potentials, known as spikes occurring at a single neuron, propagate in neuronal networks and create spatiotemporal patterns of these neuronal activities at the network level, depending on the time and location of the spikes at each neuron. These spatiotemporal patterns of neuronal activity are encoded to process information in the brains.[1] Moreover, the properties of neuronal networks, such as spatial propagation and temporal continuity of neuronal activity, are modified by external stimuli related to brain functions such as learning and memory.[2] External stimuli are known to induce altered neuronal network activities such as bursting activity, in which neuronal populations exhibit high-frequency spikes at the network-wide level.[3] Therefore, understanding the spatial propagation of neuronal electrical activity in neuronal populations in response to external stimuli is necessary to elucidate their functions in the brain.

Methods for observing neuronal activity include fluorescence Ca^{2+} imaging and electrophysiological measurement techniques such as extracellular potential recording with microelectrode arrays (MEAs) and patch-clamp recording.[4−8] Fluorescence Ca^{2+} imaging is used to visualize the intracellular Ca^{2+} distribution resulting from neuronal activity.[9−11] Electrophysiological methods have advantages in the real-time recording of neuronal electrical activity with higher temporal resolution and higher sampling rates. Extracellular potential recording using MEAs is useful for studying neuronal electrical activity at the network level over long periods of time. MEAs can also be used to stimulate neurons by injecting pulse currents into target electrodes, and the extracellular potential spikes evoked by electrical stimulation can be recorded and evaluated.[12−15] As for methods of neuronal stimulation, electrical inputs, pharmacological treatment, and optogenetic modifications have been used to understand the properties of neuronal networks in the brain, and these methods have the potential for the treatment of neurological disorders.[16,17] However, these methods have disadvantages, such as tissue invasiveness, low spatial resolution, and irreversible gene modification. Electrical stimulation offers high spatial resolution but is often tissue invasive due to electrode insertion into the cell culture.[17] Pharmacological treatments lack target specificity because of the spatial diffusion of chemicals.[18] Optogenetics using photosensitive ion channels requires irreversible gene alternation.[19] In this study, we demonstrate

Received: September 30, 2024
Revised: December 1, 2024
Accepted: December 12, 2024
Published: December 20, 2024

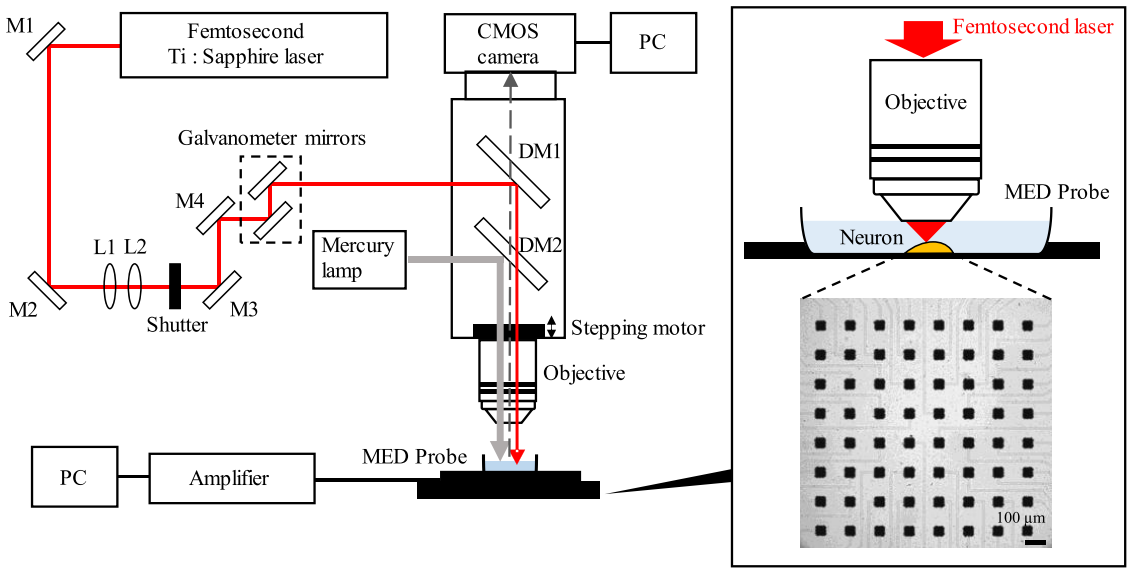

Figure 1. Experimental setup for femtosecond laser microscopy and a multisite extracellular potential recording system. M1−M4 indicate mirrors; L1 and L2 indicate lenses; DM1 and DM2 indicate dichroic mirrors. The bright-field image in the inset shows the arrangement of the 64 planar microelectrodes in the MED probe.

single-neuron stimulation in rat hippocampal neuronal networks using a focused femtosecond laser to establish a novel stimulation method with less tissue invasiveness, higher spatial resolution, and no gene modification.

The femtosecond laser has an ultrashort pulse width of the order of 10^{-15} s and is used for precise material processing induced by multiphoton absorption in the submicron focal region when focused by an objective in a microscope.[20] Femtosecond laser processing has also been applied to the nanosurgery of biological tissues such as neurons.[21−24] In previous studies, intracellular Ca^{2+} increased in femtosecond laser-irradiated neurons, and multiple neuronal electrical activities near the target neuron were confirmed by fluorescence Ca^{2+} imaging and MEAs after femtosecond laser irradiation.[23] However, network-level responses induced by femtosecond laser irradiation have not been investigated, and the differences between the spatiotemporal properties induced by femtosecond laser irradiation and those evoked by electrical stimulation remain unclear.

In this study, we investigated spatiotemporal responses in neuronal networks in response to single-neuron stimulation using a focused femtosecond laser. Neuronal activity induced by femtosecond laser irradiation was evaluated by fluorescence Ca^{2+} imaging and extracellular potential recording using MEAs, and the underlying mechanisms are discussed. In addition, conventional electrical stimulation was performed as a control experiment, and the extracellular potential spikes evoked by electrical stimulation were compared with those induced by femtosecond laser irradiation. The temporal continuity and spatial propagation of the evoked extracellular potential spikes under femtosecond laser irradiation and electrical stimulation are discussed.

2. MATERIALS AND METHODS

2.1. Cultured Rat Hippocampal Neurons. All animal procedures were approved by the Animal Care and Use Regulations of Osaka Metropolitan University. A glass-bottom dish with 27 mm-diameter coverslips (Iwaki) and MEA dishes (MED probe, Alpha MED Scientific) were used as the culture dishes. Culture dishes were coated with 0.02 v/v% polyethylenimine (PEI, Sigma-Aldrich) aqueous solution to facilitate cell adhesion to the surface on the day before cell seeding, and PEI was rinsed thrice with ultrapure water on the day of cell seeding. Hippocampal tissues were obtained from 18-day-old Wistar/ST rat embryos (Slc:Wistar/ST, Japan SLC). Tissues were treated with 6.0×10^{-2} v/v% Trypsin (Thermo Fisher Scientific) in phosphate-buffered saline (Nissui Pharmaceutical) containing 10 mM D-Glucose for 15 min at 37 °C, and then hippocampal cells were dissociated by mechanical pipetting. Cells were seeded at a density of 2.1×10^4 and 1.3×10^5 cells/cm^2 on a glass-bottom dish and the MED probe, respectively. Cells were cultured in Neurobasal Medium (Thermo Fisher Scientific) containing 2% B-27 Supplement (Thermo Fisher Scientific), 0.25% L-Glutamine (Thermo Fisher Scientific), 5 μg/mL Insulin (Sigma-Aldrich), and 1% Penicillin−Streptomycin (Pen-St, Thermo Fisher Scientific) in a glass-bottom dish and in Dulbecco's Modified Eagle Medium: Nutrient Mixture F-12 (Thermo Fisher Scientific) containing 5% heat-inactivated Fetal Bovine Serum and Horse Serum (Thermo Fisher Scientific), 5 μg/mL Insulin, and 1% Pen-St in the MED probe. The cultures were maintained at 37 °C in a 5% CO_2 incubator for 15−25 days *in vitro* (DIV). The culture medium was replaced with fresh medium twice a week.

For fluorescence Ca^{2+} imaging, neurons were loaded with the fluorescent Ca^{2+} indicator Oregon Green 488 BAPTA-1, AM (OGB-1; maximum absorption wavelength: 494 nm, maximum fluorescence emission wavelength: 523 nm; Thermo Fisher Scientific) to evaluate changes in intracellular Ca^{2+} concentrations due to femtosecond laser irradiation. A 1 mM OGB-1 dimethyl sulfoxide solution (Sigma-Aldrich) was diluted to 8 μM for the glass-bottom dish and 16 μM for the MED probe with an external solution containing 130 mM NaCl, 3 mM KCl, 2 mM $CaCl_2$, 1 mM $MgCl_2$, 10 mM HEPES, and 10 mM D-Glucose, referred to as the working solution. The extracellular Ca^{2+} concentrations in our experiments were fixed according to neuronal physiological conditions to elucidate neuronal activity without abnormal treatment.[7] The

https://doi.org/10.1021/acsomega.4c08948
ACS Omega 2025, 10, 1354−1363

working solution was sonicated for 1 min in an ultrasonic water bath (1510J-DTH, Yamato Scientific) before dye loading. The culture medium was replaced with the working solution, and the dish was incubated for 1 h. After incubation, the working solution was washed three times with the external solution, and the neurons were incubated in an external solution for 30 min. All dye-loading procedures were performed in the dark on a 37 °C hot plate (PWGX01, Cosmo Bio). To evaluate femtosecond laser-induced neuronal activity under the blockage of voltage-gated Na^+ channels, neurons were treated with tetrodotoxin (TTX; Fujifilm Wako Pure Chemical). A 1 mM TTX aqueous solution was diluted to 2 μM with an external solution and added to the neurons by exchanging half of the volume of the external solution to a final concentration of 1 μM.

2.2. Experimental Setup for Fluorescence Microscopy Imaging and Extracellular Potential Recording. The experimental setup for femtosecond laser-induced fluorescence imaging and extracellular potential recording system is shown in Figure 1.[21,23] Femtosecond Ti:sapphire laser pulses (Tsunami, Spectra-Physics) with a center wavelength of 800 nm, a pulse width of ∼100 fs, and a repetition rate of 82 MHz, were introduced into an upright fluorescence microscope (BX50WI, Olympus) and focused on a target neuron with a water immersion objective (LUMPLFLN60XW, ×60, NA 1.0, Olympus). The theoretical diameter of the laser focal spot on the sample is 0.98 μm. The laser irradiation time was set to 8 ms, with the minimum value obtained using an electromagnetic shutter (F77, Suruga Seiki). The position of the laser in the focal plane was controlled by using a pair of galvanometer mirrors in a confocal scanning unit (FV300, Olympus). The focal position of the laser was controlled using consumable software (Fluoview, Olympus). The specimens were positioned using a motorized stage (BIOS-106T-WI, Sigma Koki), and the objective was positioned along the optical axis by using a stepping motor (Olympus) with a resolution of 0.1 μm. For fluorescence Ca^{2+} imaging of neurons, excitation light from a mercury lamp (U-ULH, Olympus) passing through a bandpass filter (460−495 nm, Olympus) was used to excite the fluorescent Ca^{2+} indicator, OGB-1. To prevent photobleaching of OGB-1, a 5% neutral density filter (Olympus) was inserted in the excitation light path to set the excitation power at 150 μW at the sample level. Fluorescence was collected after passing through a dichroic mirror (>510 nm, Olympus), an absorption filter (>505 nm, Olympus), and a short-pass filter (>750 nm, Asahi Spectra). Fluorescence images were captured with a scientific complementary metal-oxide semiconductor (sCMOS) camera (ORCA-Flash4.0 V2, Hamamatsu Photonics) with a size of 2048 × 2048 pixels (240 μm × 240 μm with an objective) and a frame rate of 33.3 frames/s, and the fluorescence intensity was digitized at 16-bit resolution (maximum 65 535 counts) in each pixel.

To evaluate the changes in intracellular Ca^{2+} concentration in single neurons caused by femtosecond laser irradiation, a 102 × 102-pixel region of interest (ROI) (15 μm × 15 μm through the objective), the size of which corresponds to the cell body of a single neuron, was placed on the fluorescence images using ImageJ 1.53 (National Institute of Health). The average fluorescence intensity in the ROI of each image was calculated using a laboratory-developed Python script. The normalized fluorescence intensity $\Delta F/F$ was calculated by using the following equation.

$$\frac{\Delta F}{F} = \frac{F(t) - F_0}{F_0} \quad (1)$$

where $F(t)$ is the average fluorescence intensity at time t, and F_0 is the average fluorescence intensity of each image before laser irradiation. To detect intracellular Ca^{2+} spikes representing neuronal activity, the threshold was defined as 3 times the standard deviation of the $\Delta F/F$ values before laser irradiation. Any peak above this threshold was detected as a Ca^{2+} spike. Calculation of $\Delta F/F$ values and Ca^{2+} spike detection were performed using laboratory-developed software of LabVIEW 2011.

2.3. Extracellular Potential Recording with MEAs. The electrical activity of the neuronal networks induced by femtosecond laser irradiation was recorded by using a multisite extracellular potential recording system (MED64, Alpha MED Scientific). 64 planar Pt-black-coated microelectrodes, 50 μm × 50 μm in size, were placed in a MED probe in 8 × 8 arrays at 150 μm, as shown in Figure 1. The extracellular potentials of the neuronal network were amplified 2000-fold by a multichannel amplifier (SU-MED64, Alpha MED Scientific) and digitized at a sampling rate of 10 kHz for obtaining single spikes of single neurons and a 12-bit resolution by A/D boards (PCI-6071E, National Instruments). Electrical stimulation was performed by injecting biphasic pulse currents into a selected microelectrode with an amplitude of 1 V to 5 μA and a pulse width of 100 μs in each phase. During the electrical stimulation, the stimulation electrode was switched for current injection, and the electrical signals could not be monitored. All recording and electrical stimulation procedures were performed using the laboratory-developed LabVIEW 2011 software (National Instruments).

For the analysis, the recorded extracellular potentials were smoothed using a 10-point moving average transform and a third-order Butterworth digital bandpass filter at 100−2000 Hz. The threshold was defined as 10 times the standard deviation of the noise signals. Positive and negative peaks above and below the threshold, respectively, were detected as extracellular potential spikes representing neuronal electrical activity. In this study, stimulus artifacts due to femtosecond laser irradiation or electrical stimulation, which we defined as distortion of the extracellular potential after each operation, were excluded from spike analysis. Electrical stimulation artifacts were observed for 5 ms after current injection and were removed from the detected extracellular potential spikes at all 63 recording electrodes because the stimulation target electrode was excluded. In the case of femtosecond laser irradiation, artifacts were observed at individual electrodes adjacent to the laser-irradiated neurons. However, the spatiotemporal pattern of the observed artifacts differed between the experiments, indicating the difficulty in distinguishing artifacts from neuronal electrical activity. Therefore, during femtosecond laser irradiation, the neuronal electrical activity was evaluated by removing all extracellular potential spikes detected at the single electrode closest to the femtosecond laser-irradiated neurons. Spike detection was performed using the laboratory-developed LabVIEW 2011 software.

To compare the temporal characteristics of neuronal electrical activity induced by femtosecond laser irradiation and electrical stimulation, the number of extracellular potential spikes was calculated every 10 ms after each procedure. The spatial distribution of the detected extracellular potential spikes

https://doi.org/10.1021/acsomega.4c08948
ACS Omega 2025, 10, 1354−1363

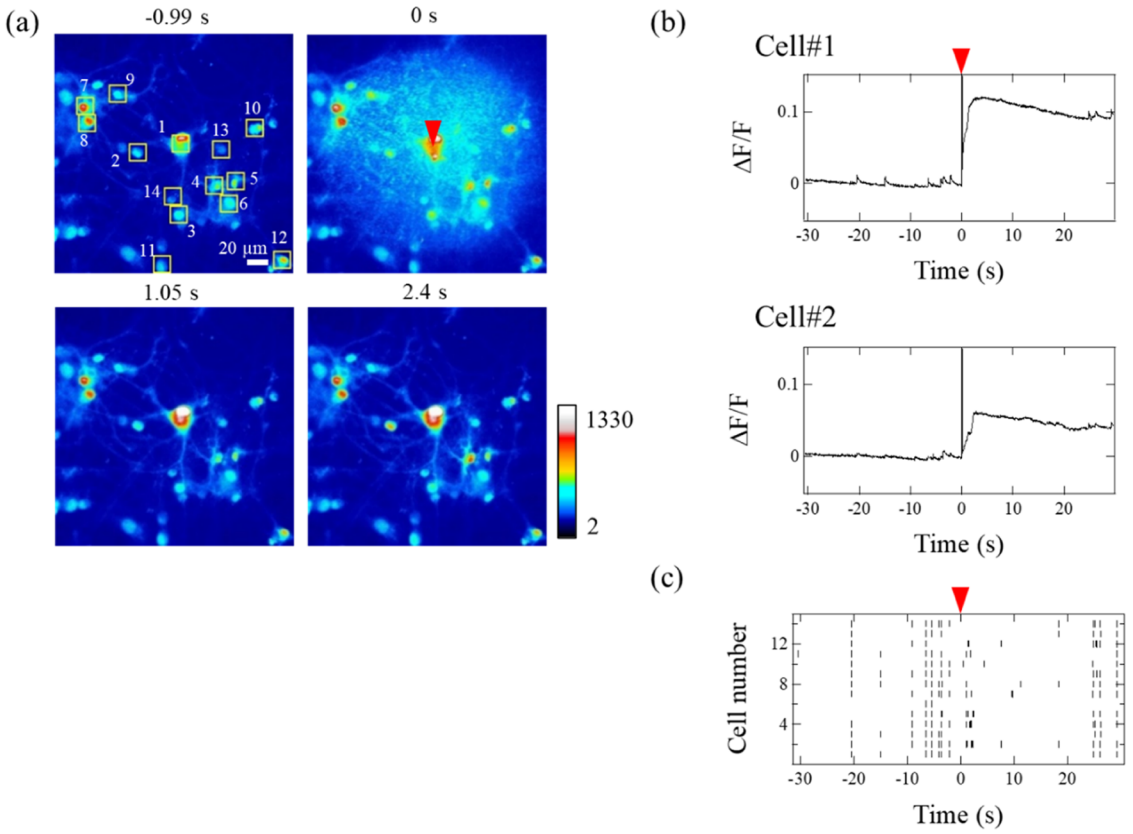

Figure 2. (a) Fluorescence images of neurons at 18 DIV loaded with OGB-1 in a glass-bottom dish before and after femtosecond laser irradiation. Yellow squares in the top left panel indicate the ROIs. The time before and after laser irradiation is shown above each image. (b) $\Delta F/F$ values for cell nos. 1 and 2. (c) Raster plot of intracellular Ca^{2+} spikes in the neurons. The red arrows indicate the laser focus and irradiation time.

was plotted to evaluate the spatial propagation of the evoked responses in both procedures. The locations of the electrodes where spikes were detected are indicated as squares, and the squares are connected with solid lines in time-sequential order after femtosecond laser irradiation or electrical stimulation, respectively. The propagation velocity of electrical activity was calculated as the maximum propagation distance of the evoked extracellular potential spikes divided by the time after stimulation. All statistical data are presented as mean ± standard error of $N = 4$ cells in two cultures.

3. RESULTS AND DISCUSSION

3.1. Fluorescence Ca^{2+} Imaging of Neurons by Femtosecond Laser Irradiation. The activity of single hippocampal neurons after femtosecond laser irradiation was evaluated by using fluorescence Ca^{2+} imaging. Figure 2a,b shows time-course fluorescence images and normalized fluorescence intensity of OGB-1-loaded neurons at 18 DIV cultured on a glass-bottom dish before and after laser irradiation, respectively. When a femtosecond laser with an average power of 30 mW and irradiation time of 8 ms was focused on the target neuron (cell no. 1 in Figure 2a), the fluorescence intensity drastically increased immediately after laser irradiation, indicating extracellular Ca^{2+} influx into the target cell. The laser power threshold for Ca^{2+} elevation at the cell body due to laser irradiation was 30 mW, which is consistent with previous results.[10] In this study, a laser power of 30 mW was used based on our previous study,[23] where intracellular Ca^{2+} elevation due to femtosecond laser irradiation had a threshold of 30 mW. The laser irradiation time was set to 8 ms, which was the minimum operation time of the mechanical shutter. Cellular damage is concerned with a higher laser power and longer irradiation time. The pulse energy of the femtosecond laser used in this study was calculated to be 0.37 nJ when calculated with an average laser power of 30 mW, which is comparable to the threshold of 0.4 nJ for femtosecond laser ablation of tissues in the previous report.[20] These data and previous reports are consistent in that femtosecond laser-induced ablation based on multiphoton absorption transiently disrupts the cell membrane in the focal region and induces extracellular Ca^{2+} to flow into the neuron owing to concentration gradients across the membrane. Extracellular Ca^{2+} entry suggests that extracellular Na^{+}, which is abundant in extracellular regions and is the cause of membrane depolarization, also flows into the target neurons by concentration gradients and generates action potentials on target neurons. Furthermore, Ca^{2+} entering the cytosol is thought to increase the membrane potential, evoking further influx through voltage-gated Ca^{2+} channels in the membrane. There is also the possibility of cytosolic Ca^{2+} elevation through Ryanodine receptors in the endoplasmic reticulum (intracellular Ca^{2+} store), known as Ca^{2+}-induced Ca^{2+} release, or through IP_3 receptors in the endoplasmic reticulum, known as IP_3-induced Ca^{2+} release.[25] In our experiments, the intracellular Ca^{2+} increase lasted for several tens of seconds following laser irradiation. This slow decay of intracellular Ca^{2+} levels may be due to neuronal Ca^{2+} buffering through Ca^{2+} ATPases in the membrane and endoplasmic reticulum with slow time constants.[26]

https://doi.org/10.1021/acsomega.4c08948
ACS Omega 2025, 10, 1354−1363

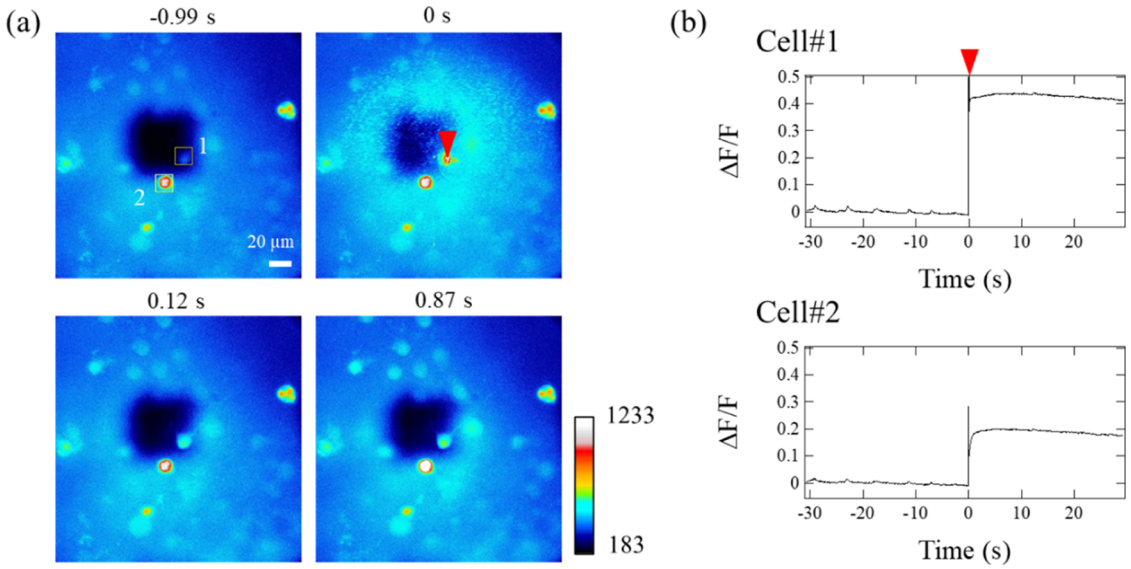

Figure 3. (a) Fluorescence images of neurons at 18 DIV loaded with OGB-1 cultured on the MED probe before and after femtosecond laser irradiation. Yellow squares indicate the ROIs. The time before and after laser irradiation is shown above each image. (b) $\Delta F/F$ values for cell nos. 1 and 2. The red arrows indicate the laser focus and irradiation time.

The fluorescence intensity also increased in the neighboring neuron (cell no. 2), as shown in Figure 2b. In Figure 2b, the drastically increased intensity at 0 s in cell nos. 1 and 2 show the scattered light of the femtosecond laser at an irradiation time of 8 ms. As shown in Figure 2c, intracellular Ca^{2+} increases in the two neurons (cell nos. 1 and 2) started at almost the same time. The synaptic conduction time between two connected neurons ranges within a few ms;[27] therefore, intracellular Ca^{2+} increases in multiple neurons can occur with almost no time lags under fluorescence imaging with an exposure time of 30 ms. Therefore, it was suggested that the two neurons (cell nos. 1 and 2 in Figure 2c) were connected via a synapse. After femtosecond laser irradiation of the target neuron (cell no. 1 in Figure 2a), highly frequent synaptic inputs from cell no. 1 can induce highly frequent neuronal activity in cell no. 2 in Figure 2a, causing a large Ca^{2+} transient by extracellular Ca^{2+} influx via voltage-gated Ca^{2+} channels and Ca^{2+} release from intracellular Ca^{2+} stores. Because femtosecond laser-induced ablation and subsequent disruption of the cell membrane occur only in the focal region based on multiphoton absorption, membrane disruption should occur only in cell no. 1. The temporal pattern of the Ca^{2+} spikes derived from fluorescence Ca^{2+} imaging is shown in Figure 2c. The drastic increase in intensity due to the scattered light of the femtosecond laser was observed for 30 ms from 0 s. The fluorescence peaks attributed to the scattered light were excluded from intracellular Ca^{2+} spike detection during femtosecond laser irradiation. These plots show that synchronized neuronal activity was induced between the target neuron and its surrounding neurons after laser irradiation. The target neuron and surrounding neurons showed spiking Ca^{2+} activity (see the $\Delta F/F$ time trace 20 s after laser irradiation in the cells of Figure 2b), indicating that the neurons were not damaged by femtosecond laser irradiation. As shown in Figure 2b, no small Ca^{2+} spikes were detected during the first 20 s after laser irradiation. Since highly frequent neuronal activity is thought to be induced in the target neuron, small Ca^{2+} spikes are buried in the large Ca^{2+} transients. The large Ca^{2+} transient is caused by extracellular Ca^{2+} influx through voltage-gated Ca^{2+} channels and Ca^{2+} release from intracellular Ca^{2+} stores such as the endoplasmic reticulum, including Ca^{2+}-induced Ca^{2+} release and IP_3-induced Ca^{2+} release. To evaluate neuronal activity due to femtosecond laser irradiation when voltage-gated Na^+ channels were blocked, the neurons were treated with TTX. Figure S1a,b show the fluorescence image and normalized fluorescence intensity of OGB-1-loaded neurons at 25 DIV before bath application of 1 μM TTX. Spiking fluorescence intensity equivalent to intracellular Ca^{2+} spikes was observed. After 20 min of bath application of TTX to neurons, these intracellular Ca^{2+} spikes disappeared, as shown in Figure S1c. These results suggest that intracellular Ca^{2+} spikes can be attributed to spontaneous action potentials. Figure S1d,e show the time-course fluorescence images and normalized fluorescence intensity of OGB-1-loaded neurons at 25 DIV after 20 min of application of 1 μM TTX. The fluorescence intensity drastically increased only in the target neuron immediately after the laser irradiation of a single neuron in the presence of TTX. Our results suggest that extracellular Ca^{2+} influx occurred through membrane disruption and was not confirmed in neighboring neurons when axonal conduction was suppressed. These results suggest that neuronal electrical activity was induced by femtosecond laser irradiation of the target neuron and then propagated to neighboring neurons.

3.2. Extracellular Potential Recordings of Femtosecond Laser-Induced Neuronal Network Activity. To evaluate femtosecond laser-induced neuronal activity, simultaneous recordings of intracellular Ca^{2+} imaging and extracellular potential recordings using MEAs were performed. To evaluate the spatiotemporal characteristics of femtosecond laser-induced neuronal electrical activity, a femtosecond laser with an average power of 30 mW and an irradiation time of 8 ms was focused on OGB-1-loaded neurons cultured in the MED probe. Note that dissociated cultured neurons at 15−25 DIV on the MED probe established synaptic connections, showing spontaneous, synchronized neuronal electrical activity at the network level.[28] Figure 3a shows the time-course fluorescence images of OGB-1-loaded neurons at 18 DIV cultured in the

https://doi.org/10.1021/acsomega.4c08948
ACS Omega 2025, 10, 1354−1363

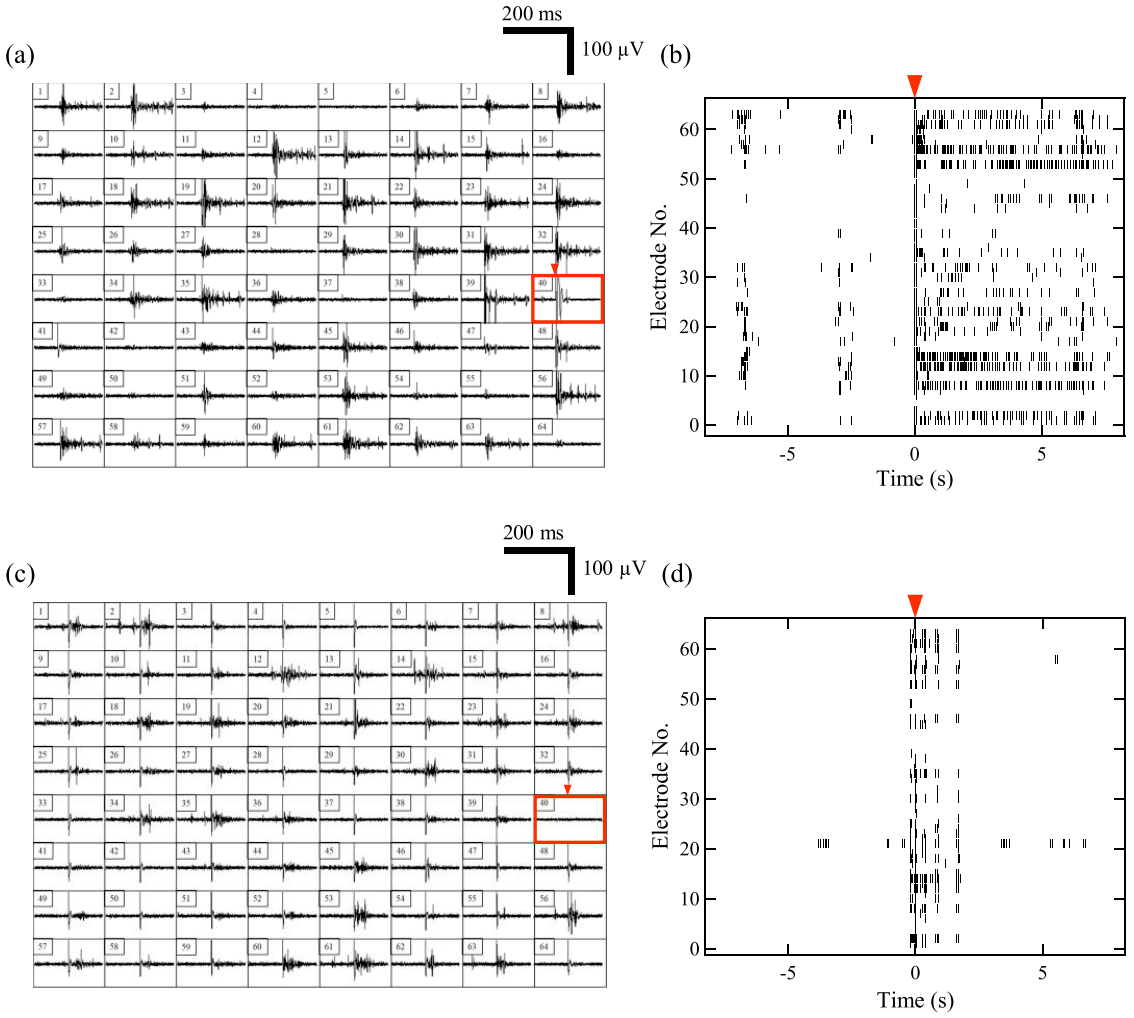

Figure 4. (a, c) Extracellular potentials of the 64 microelectrodes induced by femtosecond laser irradiation (a) and electrical stimulation (c). (b, d) Raster plots of extracellular potential spikes of neurons at 18 DIV induced by femtosecond laser irradiation (b) and those evoked by electrical stimulation (d). The 0 s indicates the time point of the femtosecond laser irradiation and electrical input. The red squares and arrows indicate the stimulation site and laser irradiation time, respectively.

MED probe before and after femtosecond laser irradiation. The normalized fluorescence intensity increased drastically in the target neuron (cell no. 1 in Figure 3a) and neighboring neuron (cell no. 2 in Figure 3a), as shown in Figure 3b. This result suggests that an influx of extracellular Ca^{2+} was also induced in target neurons cultured in the MED probe. The evoked responses due to femtosecond laser irradiation were evaluated by extracellular potential recording using MED probes. The extracellular potentials of the 64 planar microelectrodes were simultaneously recorded before and after laser irradiation, as shown in Figure 4a. A femtosecond laser was focused on the target neuron adjacent to electrode no. 40. The spike patterns for 10 s before and after laser irradiation are shown in Figure 4b. The average extracellular potential spikes increased for 5 s from 333.5 to 765.8 spikes before and after femtosecond laser irradiation ($N = 4$ cells in two cultures), and the average increase rate was 2.67 ± 0.71. These results indicate that high-frequency neuronal electrical activity was induced by femtosecond laser irradiation.

3.3. Femtosecond Laser-Induced Neuronal Electrical Activity Compared with Those Evoked by Electrical Stimulation. To compare the electrical activity characteristics between those induced by femtosecond laser irradiation and those evoked by conventional electrical stimulation, a biphasic pulse current with an amplitude of 5 μA and pulse width of 100 μs was injected into stimulation electrode no. 40, which was adjacent to the neuron irradiated by the femtosecond laser. In previous reports using conventional electrical stimulation, biphasic pulse current was injected into the stimulation electrode for 100 μs to avoid charge saturation in the electrical measurement field.[5,15,29] In MED probes, extracellular potentials around the stimulation electrode are modulated by injecting a biphasic pulse current through a microelectrode and depolarization of membrane potentials is induced in some neurons surrounding the stimulation electrode. The duration of the current injection is much shorter compared to the time scale of action potential generation, but this duration of inputs is sufficient to induce a single action potential in the neurons.[5,15,30] The extracellular potentials before and after electrical stimulation are shown in Figure 4c. As shown in Figure 4c, the target electrode (electrode no. 40) showed no signals because it was used for current injection. Note that spontaneous synchronized electrical activity was observed before laser irradiation or current injection since dissociated cultured neurons formed synaptic connections on the MED probes. The extracellular potential spike patterns for 10 s

https://doi.org/10.1021/acsomega.4c08948
ACS Omega 2025, 10, 1354−1363

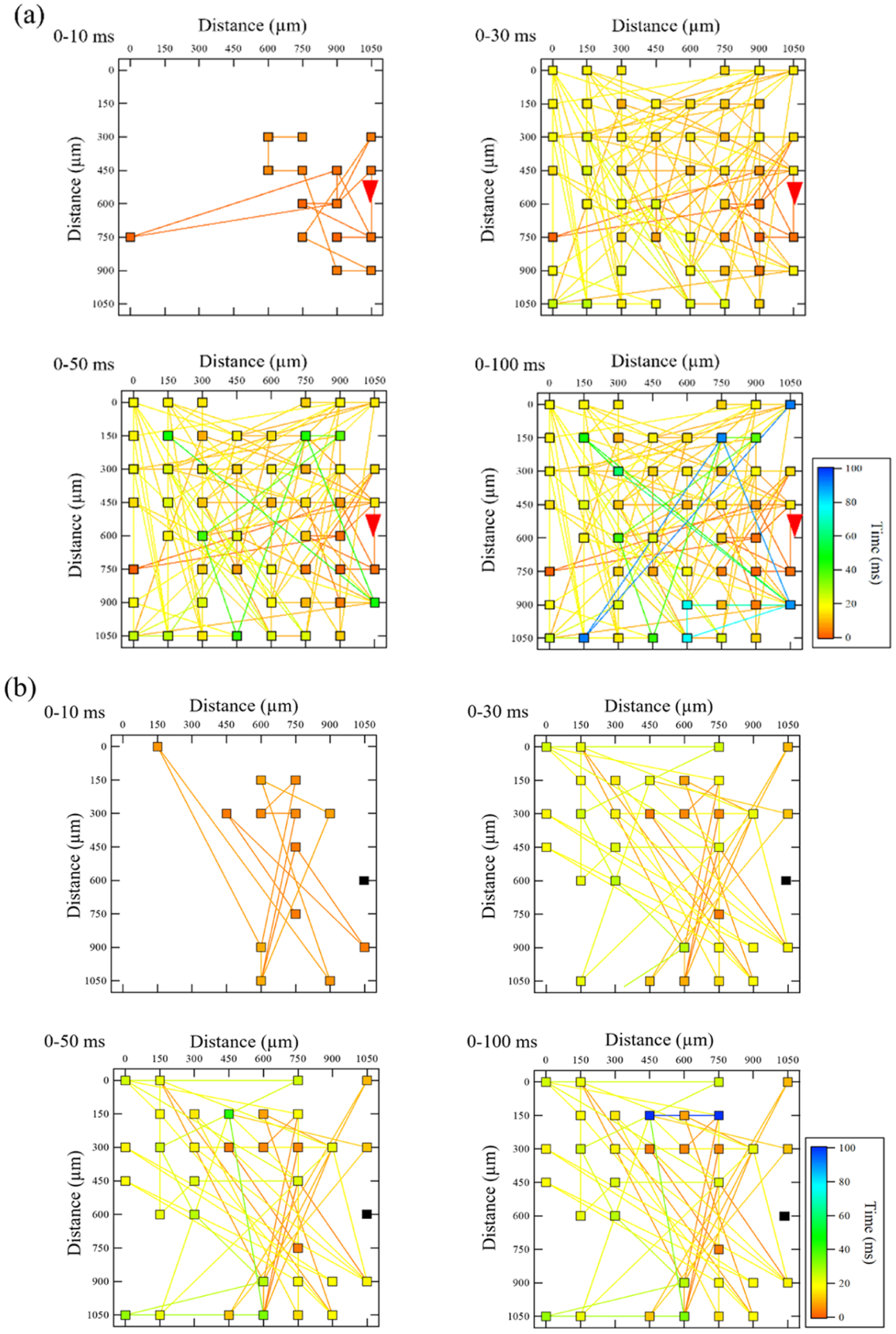

Figure 5. Spatial distribution of extracellular potential spikes in the entire area of the 64 electrodes after 10, 30, 50, and 100 ms after femtosecond laser irradiation (a) and electrical stimulation (b). Red arrows and squares indicate the stimulation sites. Black squares indicate the locations of the stimulation electrodes. Each square is 50 μm × 50 μm in size.

https://doi.org/10.1021/acsomega.4c08948
ACS Omega 2025, 10, 1354−1363

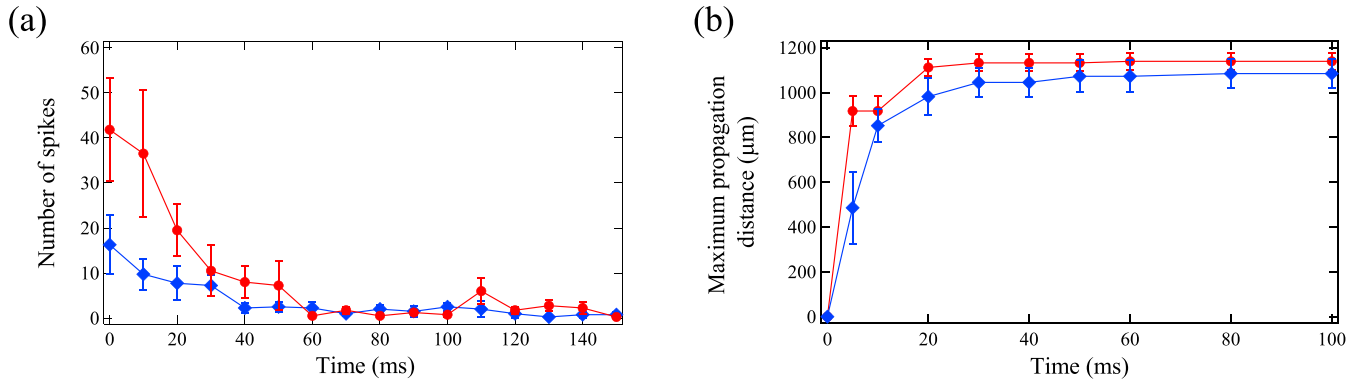

Figure 6. (a) Time course of the number of extracellular potential spikes every 10 ms after femtosecond laser irradiation (red line) and electrical stimulation (blue line). (b) Maximum propagation distances of the electrical spikes after femtosecond laser irradiation (red line) and electrical stimulation (blue line).

before and after electrical stimulation are shown in Figure 4d. As shown in Figure 4d, the extracellular potential spikes observed before electrical stimulation were due to spontaneous neuronal activity. The neuronal responses were observed immediately after electrical stimulation for several tens of milliseconds, which is comparable to the duration of evoked neuronal activity in a previous study.[15] The average extracellular potential spikes increased for 5 s from 236.0 to 348.8 spikes before and after electrical stimulation (N = 4 cells in two cultures), and the average increase rate was 1.62 ± 0.25. These results indicate that neuronal electrical activity was also evoked by conventional electrical stimulation, and that high-frequency electrical activity was maintained after electrical stimulation.

The spatial propagation of extracellular potential spikes induced by femtosecond laser irradiation and those evoked by electrical stimulation was evaluated. The locations of the electrodes where electrical spikes were detected 10, 30, 50, and 100 ms after each operation are shown in Figure 5. Each panel shows a snapshot at the time written on the top left from the time of the laser irradiation at 0 s. Neuronal electrical activity propagated up to 917 ± 68, 1131 ± 38, 1139 ± 39, and 1139 ± 39 μm (N = 4 irradiations in two cultures) in the case of femtosecond laser irradiation, and 485 ± 159, 981 ± 81, 1072 ± 70, and 1084 ± 65 μm (N = 4 stimuli in two cultures) in the case of electrical stimulation at 10, 30, 50, and 100 ms after each operation, respectively. The propagation velocity of the electrical activity was estimated to be 51.57 ± 17.50 μm/ms (N = 4 irradiations in two cultures) in the case of femtosecond laser irradiation and 39.57 ± 9.93 μm/ms (N = 4 irradiations in two cultures) in the case of electrical stimulation. We confirmed that there were no significant differences between the two operations using Welch's t test. Note that this velocity indicates the spike detection time after femtosecond laser irradiation in other electrodes divided by the distance from the laser focal region or electrical input point and is not correlated with the synaptic transmission (conduction) velocity. This slightly faster propagation is probably due to the steeper membrane potential elevation in femtosecond laser irradiation than that in conventional electrical stimulation. These results suggest that the extracellular potential spikes induced by femtosecond laser irradiation or those evoked by electrical stimulation propagated further away from the sites of laser irradiation or the stimulation electrode over time and that the former propagated faster to farther regions than the latter.

The temporal characteristics of the evoked extracellular potential spikes were compared between femtosecond laser irradiation and electrical stimulation. The increase ratios of the spike rates before and after laser irradiation were higher than those after electrical stimulation. In addition, the duration of the evoked extracellular potential spikes differed between the two methods. The time course of the spike rate every 10 ms after each operation is shown in Figure 6a. The evoked responses lasted for 60 and 40 ms after femtosecond laser irradiation and electrical stimulation, respectively. These results indicate that femtosecond laser irradiation at the average power of 30 mW and irradiation time of 8 ms induces more neuronal spikes than a single electrical stimulation. In the present study, Ca^{2+} transients lasted for several tens of seconds after femtosecond laser irradiation and highly frequent extracellular potential spikes lasted for 60 ms after laser irradiation. Extracellular potential spikes reflect collective neuronal activity around the recording electrodes; however, fluorescence Ca^{2+} imaging allows us to assess individual neuronal activity. Therefore, the two recording paradigms have different temporal resolutions, leading to different durations of femtosecond laser-induced neuronal activity.

The maximum propagation distance of the evoked extracellular potential spikes at each time point after each operation is shown in Figure 6b. Evoked responses induced by femtosecond laser irradiation and electrical stimulation were propagated from the sites of the laser irradiation and stimulation electrodes. It is suggested that the neuronal electrical activity induced by femtosecond laser irradiation propagates faster to more distant neurons than that evoked by electrical stimulation. Therefore, more electrical spikes can be observed in evoked responses with femtosecond laser irradiation under our experimental conditions at an average power of 30 mW and irradiation time of 8 ms compared to electrical stimulation because a larger number of neurons are activated by synaptic transmission from the target neurons. These results suggest that the spatiotemporal pattern of neuronal activity, such as neuronal synchrony and bursting activity,[6,31,32] can be modulated by femtosecond laser irradiation. This quantitative analysis will be effective for clarifying the effects of femtosecond laser irradiation on neuronal encoding.

3.4. Mechanisms of Neuronal Stimulation between Femtosecond Laser Irradiation and Electrical Stimulation. Here, we discuss the mechanisms underlying the

https://doi.org/10.1021/acsomega.4c08948
ACS Omega 2025, 10, 1354−1363

induction of neuronal activity by femtosecond laser irradiation and electrical stimulation, which contribute to the different characteristics of the evoked electrical activity. When a femtosecond laser is focused on a target neuron, transient disruption of the cell membrane occurs in the focal region, induced by femtosecond laser ablation based on multiphoton absorption, as described in our previous study.[23] This disruption induces the influx of extracellular Na^+ through concentration gradients across the membrane and depolarization of the membrane potential, thereby generating action potentials. Femtosecond laser-induced membrane disruption was previously reported to heal within a few seconds after femtosecond laser irradiation at a center wavelength of 800 nm, pulse width of ∼100 fs, and repetition rate of 80 MHz on MCF7 cell surfaces by fluorescence analysis.[33] Therefore, the transient membrane disruption caused by femtosecond laser irradiation is expected to recover within a few seconds in our experiments. The neurons showed spiking behavior after transient disruption and recovery of the cell membrane, indicating that cell viability was maintained, as shown in Figure 2. In the presence of membrane disruption, the upstate membrane potentials are sustained for a few seconds and multiple action potentials are induced. Transient membrane disruption is thought to be recovered by lateral diffusion of the membrane from outside the focal region.[33] However, the large Ca^{2+} transients lasted for several tens of seconds after femtosecond laser irradiation, as shown in Figure 2b. Because intracellular Ca^{2+} buffering takes a longer time after extracellular Ca^{2+} influx, the high concentration persists for tens of seconds after membrane recovery. Fluorescence Ca^{2+} imaging and extracellular potential recordings are not sufficient to evaluate electrophysiological properties at the level of individual target neurons because of the limited spatiotemporal resolution of extracellular potential recordings and the indirect evaluation of neuronal electrical activity in Ca^{2+} imaging. Detailed electrophysiological mechanisms of femtosecond laser-induced neuronal stimulation should be investigated in the future using electrophysiological recordings at the single-cell level.[34−36]

As described above, in the case of femtosecond laser-induced stimulation, membrane depolarization is expected to persist for a longer period than that evoked by electrical stimulation, owing to transient membrane disruption. Therefore, femtosecond laser irradiation may induce a longer-lasting, larger number of neuronal spikes and more widespread neuronal electrical activity with lower invasiveness and a higher spatial accuracy at the single-cell level than conventional electrical stimulation.

In this study, we confirmed the reproducibility in the number of femtosecond laser-induced neuronal activities in the neuronal network. The neuronal activity in femtosecond laser-irradiated neurons can be further investigated by using patch-clamp recordings. Our proposed neuronal stimulation methods have limitations in stimulation frequency since transient disruption of the membrane is thought to recover within a few seconds, resulting in a single stimulation. This limitation can be improved by optimizing the femtosecond laser parameters, such as the laser irradiation time, using an acousto-optic modulator.

4. CONCLUSIONS

We demonstrated single-neuron stimulation using a focused femtosecond laser in cultured rat hippocampal neurons and evaluated the induced neuronal activity by using fluorescence Ca^{2+} imaging and extracellular potential recordings. After 8 ms of femtosecond laser irradiation, intracellular Ca^{2+} elevation was confirmed in a single target neuron, which was associated with sustained high-frequency extracellular potentials. Femtosecond laser-induced neuronal responses elicited more extracellular potential spikes, lasted longer, and propagated among neuronal networks larger than those elicited by conventional current injections. Upstate membrane potentials due to submicrometer membrane disruption are considered to induce highly frequent neuronal spikes during femtosecond laser irradiation. These results suggest that femtosecond laser irradiation is effective in directly stimulating neuronal networks at the single-cell level. Femtosecond laser stimulation may be a promising tool that can be applied to single-neuron stimulation to facilitate the investigation of neuronal information processing systems in the brain at the single-cell level.

■ ASSOCIATED CONTENT

Supporting Information

The Supporting Information is available free of charge at https://pubs.acs.org/doi/10.1021/acsomega.4c08948.

Intracellular Ca^{2+} elevation due to femtosecond laser irradiation on neurons in the presence of TTX. (PDF)

■ AUTHOR INFORMATION

Corresponding Author

Chie Hosokawa − *Department of Chemistry, Graduate School of Science, Osaka Metropolitan University, Osaka 558-8585, Japan;* orcid.org/0000-0002-0289-4680; Email: hosokawa@omu.ac.jp

Authors

Yumi Segawa − *Department of Chemistry, Graduate School of Science, Osaka Metropolitan University, Osaka 558-8585, Japan;* orcid.org/0009-0002-0629-3521

Wataru Minoshima − *Department of Chemistry, Graduate School of Science, Osaka Metropolitan University, Osaka 558-8585, Japan; Kobe Frontier Research Center, Advanced ICT Research Institute, National Institute of Information and Communications Technology, Kobe 651-2492, Japan*

Kyoko Masui − *Department of Chemistry, Graduate School of Science, Osaka Metropolitan University, Osaka 558-8585, Japan;* orcid.org/0000-0002-5065-3021

Complete contact information is available at: https://pubs.acs.org/10.1021/acsomega.4c08948

Notes

The authors declare no competing financial interest.

■ ACKNOWLEDGMENTS

This work was supported by the JSPS KAKENHI Grants-in-Aid (Grant Nos. JP22H05140, JP23K18511, and JP23K28191), Asahi Glass Foundation, and JST FOREST Program (Grant No. JPMJFR2053).

■ REFERENCES

(1) Herculano-Houzel, S. The human brain in numbers: a linearly scaled-up primate brain. *Front. Hum. Neurosci.* **2009**, *3*, 31.

(2) Lamprecht, R.; LeDoux, J. Structural Plasticity and Memory. *Nat. Rev. Neurosci.* **2004**, *5* (1), 45−54.

(3) Jimbo, Y.; Kawana, A.; Parodi, P.; Torre, V. The Dynamics of a Neuronal Culture of Dissociated Cortical Neurons of Neonatal Rats. *Biol. Cybern.* **2000**, *83* (1), 1−20.
(4) Gross, G. W.; Rieske, E.; Kreutzberg, G. W.; Meyer, A. A New Fixed-Array Multi-Microelectrode System Designed for Long-Term Monitoring of Extracellular Single Unit Neuronal Activity in Vitro. *Neurosci. Lett.* **1977**, *6* (2−3), 101−105.
(5) Jimbo, Y.; Tateno, T.; Robinson, H. P. Simultaneous Induction of Pathway-Specific Potentiation and Depression in Networks of Cortical Neurons. *Biophys. J.* **1999**, *76* (2), 670−678.
(6) Chiappalone, M.; Bove, M.; Vato, A.; Tedesco, M.; Martinoia, S. Dissociated Cortical Networks Show Spontaneously Correlated Activity Patterns during in Vitro Development. *Brain Res.* **2006**, *1093* (1), 41−53.
(7) Minoshima, W.; Masui, K.; Tani, T.; Nawa, Y.; Fujita, S.; Ishitobi, H.; Hosokawa, C.; Inouye, Y. Deuterated Glutamate-Mediated Neuronal Activity on Micro-Electrode Arrays. *Micromachines* **2020**, *11* (9), No. 830, DOI: 10.3390/mi11090830.
(8) Isomura, T.; Kotani, K.; Jimbo, Y.; Friston, K. J. Experimental Validation of the Free-Energy Principle with in Vitro Neural Networks. *Nat. Commun.* **2023**, *14* (1), No. 4547.
(9) Takeoka, S.; Fujii, M.; Hayashi, S.; Yamamoto, K. Size-Dependent near-Infrared Photoluminescence from Ge Nanocrystals Embedded in SiO_2 Matrices. *Phys. Rev. B* **1998**, *58* (12), 7921−7925.
(10) Ikegaya, Y.; Aaron, G.; Cossart, R.; Aronov, D.; Lampl, I.; Ferster, D.; Yuste, R. Synfire Chains and Cortical Songs: Temporal Modules of Cortical Activity. *Science* **2004**, *304* (5670), 559−564.
(11) Ota, K.; Oisi, Y.; Suzuki, T.; Ikeda, M.; Ito, Y.; Ito, T.; Uwamori, H.; Kobayashi, K.; Kobayashi, M.; Odagawa, M.; Matsubara, C.; Kuroiwa, Y.; Horikoshi, M.; Matsushita, J.; Hioki, H.; Ohkura, M.; Nakai, J.; Oizumi, M.; Miyawaki, A.; Aonishi, T.; Ode, T.; Murayama, M. Fast, Cell-Resolution, Contiguous-Wide Two-Photon Imaging to Reveal Functional Network Architectures across Multi-Modal Cortical Areas. *Neuron* **2021**, *109* (11), 1810−1824.e9.
(12) Oka, H.; Shimono, K.; Ogawa, R.; Sugihara, H.; Taketani, M. A New Planar Multielectrode Array for Extracellular Recording: Application to Hippocampal Acute Slice. *J. Neurosci. Methods* **1999**, *93* (1), 61−67.
(13) Beggs, J. M.; Plenz, D. Neuronal Avalanches in Neocortical Circuits. *J. Neurosci.* **2003**, *23* (35), 11167−11177.
(14) Suzuki, I.; Yasuda, K. Detection of Tetanus-Induced Effects in Linearly Lined-up Micropatterned Neuronal Networks: Application of a Multi-Electrode Array Chip Combined with Agarose Microstructures. *Biochem. Biophys. Res. Commun.* **2007**, *356* (2), 470−475.
(15) Jimbo, Y.; Kasai, N.; Torimitsu, K.; Tateno, T.; Robinson, H. P. C. A System for MEA-Based Multisite Stimulation. *IEEE Trans. Biomed. Eng.* **2003**, *50* (2), 241−248.
(16) Sepinwall, J. Cholinergic Stimulation of the Brain and Avoidance Behavior. *Psychon. Sci.* **1966**, *5* (3), 93−94.
(17) Chen, M.; Bi, L.-L. Optogenetic Long-Term Depression Induction in the PVT-CeL Circuitry Mediates Decreased Fear Memory. *Mol. Neurobiol.* **2019**, *56* (7), 4855−4865.
(18) Tufail, Y.; Matyushov, A.; Baldwin, N.; Tauchmann, M. L.; Georges, J.; Yoshihiro, A.; Tillery, S. I. H.; Tyler, W. J. Transcranial Pulsed Ultrasound Stimulates Intact Brain Circuits. *Neuron* **2010**, *66* (5), 681−694.
(19) Szobota, S.; Gorostiza, P.; Del Bene, F.; Wyart, C.; Fortin, D. L.; Kolstad, K. D.; Tulyathan, O.; Volgraf, M.; Numano, R.; Aaron, H. L.; Scott, E. K.; Kramer, R. H.; Flannery, J.; Baier, H.; Trauner, D.; Isacoff, E. Y. Remote Control of Neuronal Activity with a Light-Gated Glutamate Receptor. *Neuron* **2007**, *54* (4), 535−545.
(20) Vogel, A.; Noack, J.; Hüttman, G.; Paltauf, G. Mechanisms of Femtosecond Laser Nanosurgery of Cells and Tissues. *Appl. Phys. B* **2005**, *81*, 1015−1047.
(21) Hosokawa, C.; Kudoh, S. N.; Kiyohara, A.; Hosokawa, Y.; Okano, K.; Masuhara, H.; Taguchi, T. Femtosecond Laser Modification of Living Neuronal Network. *Appl. Phys. A* **2008**, *93* (1), 57−63.
(22) Liu, X.; Lv, X.; Zeng, S.; Zhou, W.; Luo, Q. Noncontact and Nondestructive Identification of Neural Circuits with a Femtosecond Laser. *Appl. Phys. Lett.* **2009**, *94* (6), No. 061113.
(23) Hosokawa, C.; Sakamoto, Y.; Kudoh, S. N.; Hosokawa, Y.; Taguchi, T. Femtosecond Laser-Induced Stimulation of a Single Neuron in a Neuronal Network. *Appl. Phys. A* **2013**, *110*, 607−612, DOI: 10.1007/s00339-012-7137-6.
(24) Hosokawa, C.; Kudoh, S. N.; Kiyohara, A.; Taguchi, T. Resynchronization in Neuronal Network Divided by Femtosecond Laser Processing. *NeuroReport* **2008**, *19* (7), 771−775.
(25) Kostyuk, P.; Verkhratsky, A. Calcium Stores in Neurons and Glia. *Neuroscience* **1994**, *63* (2), 381−404.
(26) Blaustein, M. P. Calcium Transport and Buffering in Neurons. *Trends Neurosci.* **1988**, *11* (10), 438−443.
(27) Sabatini, B. L.; Regehr, W. G. Timing of Synaptic Transmission. *Annu. Rev. Physiol.* **1999**, *61* (1), 521−542.
(28) Biffi, E.; Regalia, G.; Menegon, A.; Ferrigno, G.; Pedrocchi, A. The Influence of Neuronal Density and Maturation on Network Activity of Hippocampal Cell Cultures: A Methodological Study. *PLoS One* **2013**, *8* (12), No. e83899.
(29) Merrill, D. R.; Bikson, M.; Jefferys, J. G. R. Electrical Stimulation of Excitable Tissue: Design of Efficacious and Safe Protocols. *J. Neurosci. Methods* **2005**, *141* (2), 171−198.
(30) Wagenaar, D. A.; Pine, J.; Potter, S. M. Effective Parameters for Stimulation of Dissociated Cultures Using Multi-Electrode Arrays. *J. Neurosci. Methods* **2004**, *138* (1−2), 27−37.
(31) van Pelt, J.; Wolters, P. S.; Corner, M. A.; Rutten, W. L. C.; Ramakers, G. J. A. Long-Term Characterization of Firing Dynamics of Spontaneous Bursts in Cultured Neural Networks. *IEEE Trans. Biomed. Eng.* **2004**, *51* (11), 2051−2062.
(32) Howard, M. W.; Eichenbaum, H. Time and Space in the Hippocampus. *Brain Res.* **2015**, *1621*, 345−354.
(33) Waleed, M.; Hwang, S.-U.; Kim, J.-D.; Shabbir, I.; Shin, S.-M.; Lee, Y.-G. Single-Cell Optoporation and Transfection Using Femtosecond Laser and Optical Tweezers. *Biomed. Opt. Express* **2013**, *4* (9), 1533−1547.
(34) Chiovini, B.; Pálfi, D.; Majoros, M.; Juhász, G.; Szalay, G.; Katona, G.; Szőri, M.; Frigyesi, O.; Lukácsné Haveland, C.; Szabó, G.; Erdélyi, F.; Máté, Z.; Szadai, Z.; Madarász, M.; Dékány, M.; Csizmadia, I. G.; Kovács, E.; Rózsa, B.; Mucsi, Z. Theoretical Design, Synthesis, and In Vitro Neurobiological Applications of a Highly Efficient Two-Photon Caged GABA Validated on an Epileptic Case. *ACS Omega* **2021**, *6* (23), 15029−15045.
(35) Gong, B.; Liu, M.; Qi, Z. Membrane Potential Dependent Duration of Action Potentials in Cultured Rat Hippocampal Neurons. *Cell. Mol. Neurobiol.* **2008**, *28* (1), 49−56.
(36) Mendonça, P. R.; Vargas-Caballero, M.; Erdélyi, F.; Szabó, G.; Paulsen, O.; Robinson, H. P. C. Stochastic and Deterministic Dynamics of Intrinsically Irregular Firing in Cortical Inhibitory Interneurons. *eLife* **2016**, *5*, No. e16475.

https://doi.org/10.1021/acsomega.4c08948
ACS Omega 2025, 10, 1354−1363